Kinetic Characterization of the Catalytic Mechanism of Methionine Sulfoxide Reductase B from *Neisseria meningitidis*†

Alexandre Olry, Sandrine Boschi-Muller, and Guy Branlant*

UMR 7567 CNRS-UHP, Maturation of ARN and Molecular Enzymology, Faculty of Sciences, Boulevard des Aiguillettes, BP 239, 54506 Vandoeuvre-lès-Nancy, France

Received April 7, 2004; Revised Manuscript Received June 9, 2004

ABSTRACT: Methionine sulfoxide reductases catalyze the thioredoxin-dependent reduction of methionine sulfoxide back to methionine. The methionine sulfoxide reductases family is composed of two structurally unrelated classes of enzymes named MsrA and MsrB, which display opposite stereoselectivities toward the sulfoxide function. Both enzymes are monomeric and share a similar three-step chemical mechanism. First, in the reductase step, a sulfenic acid intermediate is formed with a concomitant release of 1 mol of methionine per mol of enzyme. Then, an intradisulfide bond is formed. Finally, Msrs return back to reduced forms via reduction by thioredoxin. In the present study, it is shown for the *Neisseria meningitidis* MsrB that (1) the reductase step is rate-determining in the process leading to formation of the disulfide bond and (2) the thioredoxin-recycling process is rate-limiting. Moreover, the data suggest that within the thioredoxin-recycling process, the rate-limiting step takes place after the two-electron chemical exchange and thus is associated with the release of oxidized thioredoxin.

Oxidation of proteins can readily occur during oxidative stress conditions by reactive oxygen species (ROS). One of the targets in proteins is a methionine (Met) residue, which can be oxidized into methionine sulfoxide (MetSO).[1] Met oxidation is reversed in vivo by methionine sulfoxide reductases (Msr). Two classes of Msrs called MsrA and MsrB have been described so far, which reduce free and protein-bound MetSO back to Met, using reduced thioredoxin (Trx) as an electron source (*1*−*6*). Three major roles for Msrs have been postulated: they can (1) scavenge ROS species such as an antioxidant molecule (*7*, *8*), (2) repair oxidized proteins and therefore may regulate the function of these proteins (*9*, *10*), and (3) play a role in the virulence of some bacteria (*11*−*14*).

MsrA and MsrB are two structurally unrelated classes of enzymes that display opposite stereoselectivities toward the S and R isomers of the sulfoxide function of MetSO, respectively (*2*−*6*). The 3-D structures of MsrA from *Escherichia coli*, *Bos taurus*, and *Mycobacterium tuberculosis* and of MsrB from *Neisseria gonorrhoeae* and *N. meningitidis* were determined by X-ray crystallography (*15*−*19*). The structure of MsrA is of mixed α−*β*-type with an active site, which can be described as an opening basin readily accessible to the substrate. This site contains the catalytic Cys-51 located at the N-terminus of an α-helix. The core of the MsrB structure is composed of two antiparallel *β*-sheets, and the active site is also solvent exposed and contains the catalytic Cys-117 located in the middle of a *β*-strand. Except for the presence of the catalytic and the recycling cysteines and of a tryptophan, the latter of which is involved in the recognition of the methyl of the sulfoxide substrate, the two active sites do not share any other common amino acids that can be involved either in the chemical mechanism or in the substrate specificities. However, both classes of Msrs share the same three-step chemical mechanism including (1) a nucleophilic attack of the catalytic Cys residue on the sulfur atom of the sulfoxide substrate leading via a 1,3-sigmatropic rearrangement to formation of a sulfenic acid intermediate and release of 1 mol of Met per mol of enzyme, (2) a formation of an intramonomeric disulfide bond between the catalytic and the recycling cysteines with a concomitant release of 1 mol of water, and (3) a reduction of the Msr disulfide bond by Trx leading to regeneration of the reduced form of Msr and to formation of oxidized Trx in the disulfide state (Trx_{ox}) (Scheme 1) (*6*, *20*). For MsrA, this chemical mechanism is in agreement with the kinetic mechanism, which was shown to be of ping−pong type (*21*).

Recent studies from our group on the catalytic mechanism of the MsrA from *N. meningitidis* have shown that the rate-limiting step is associated with the reduction of the MsrA disulfide bond by Trx and that the rate of the sulfenic acid intermediate formation is fast and is rate-determining in the process leading to formation of the MsrA disulfide bond (*22*). In contrast, no data are presently available on the kinetics of the MsrBs.

† This research was supported by the Centre National de la Recherche Scientifique (Programme Physique et Chimie du Vivant 2000, Programme Protéomique et Génie des Protéines 2001), the University Henri Poincaré Nancy I, the Association pour la Recherche sur le Cancer (Association pour la Recherche sur le Cancer Grant 5436), and the Institut Fédératif de Recherches 111 Bioingénierie.

* Corresponding author. Phone: (33) 3 83 68 43 04; fax: (33) 3 83 68 43 07; e-mail: guy.branlant@maem.uhp-nancy.fr.

[1] Abbreviations: MetSO, methionine sulfoxide; DTNB, 5,5′-dithiobis(2-nitro)benzoate; MES, 2(*N*-morpholino)ethanesulfonic acid; MsrA/B, methionine sulfoxide reductase A/B; Trx, thioredoxin; $MsrB_{ox}$, MsrB in the disulfide state; $MsrB_{red}$, MsrB in the reduced state; Trx_{ox}, Trx in the disulfide state; Trx_{red}, Trx in the reduced state.

10.1021/bi049306z CCC: $27.50
Published on Web 08/20/2004

Scheme 1: Proposed Catalytic Mechanism of MsrA and MsrB from *N. meningitidis*[a]

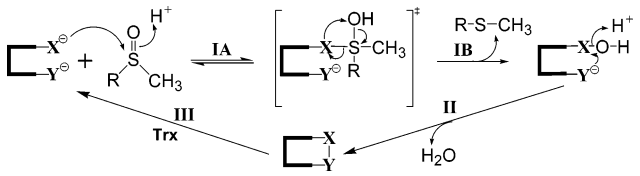

[a] Representation of the three-step chemical mechanism as described by Antoine et al. (*22*). In step III, a Michaelis complex is formed between Msr_{ox} and Trx_{red}. Then, a nucleophilic attack of Cys-32 of Trx on the disulfide bond of the Msr leads to formation of an intermolecular disulfide bond, which is followed by a nucleophilic attack of Cys-35 of Trx that leads to Msr_{red} and Trx_{ox}. For MsrB from *N. meningitidis*, X represents Cys-117 and Y Cys-63.

In the present study, the rates of the three steps of the chemical mechanism have been determined for the *N. meningitidis* MsrB. The results demonstrate that the Trx-recycling process is rate limiting. The data also suggest that within the Trx-recycling process, the rate-limiting step takes place after the two-electron chemical exchange and thus is associated with the release of Trx_{ox}. These results are compared with those recently described for MsrA (*22*).

EXPERIMENTAL PROCEDURES

Site-Directed Mutagenesis, Production, and Purification of Enzymes. The *E. coli* strain used for all *N. meningitidis* MsrB productions was BE002 (MG1655 msrA::specΩ, msrB::α3kan), transformed with the plasmidic construction pSKPILBMsrB containing the coding sequence of *msrB* under the *lac* promoter (*6*). The BE002 strain was kindly provided by Dr. F. Barras. Its use prevented expression of endogenous wild-type MsrA and MsrB from *E. coli* and thus avoided any contamination of the activity of the *N. meningitidis* MsrB by the Msrs from *E. coli*. Site-directed mutageneses were performed using the QuikChange site-directed mutagenesis kit (Stratagene).

Purifications were realized as described previously (*6*). Purity of wild-type and mutant MsrBs was checked by electrophoresis on 15% SDS−PAGE gel followed by Coomassie Brilliant Blue R-250 staining and by electrospray mass spectrometry analyses. Storage of the enzymes was done as described previously (*6*). The molecular concentration was determined spectrophotometrically, using an extinction coefficient at 280 nm of 17 330 M^{-1} cm^{-1} for wild-type and mutant MsrBs (*6*). In this paper, *N. meningitidis* MsrB amino acid numbering is based on the *E. coli* MsrB sequence without the N-terminal Met.

Trx1 and Trx reductase from *E. coli* were prepared following experimental procedures already published (*23*, *24*).

Preparation of Ac-L-Met-R,S-SO-NHMe. Ac-L-Met-OMe was purchased from Bachem. Treatment of Ac-L-Met-OMe with 25 mol equiv of methylamine in methanol gave Ac-L-Met-NHMe. Oxidation of Ac-L-Met-NHMe with 1.05 mol equiv of H_2O_2 in methanol resulted in Ac-L-Met-*R,S*-SO-NHMe. Separation of Ac-L-Met-*R,S*-SO-NHMe from residual nonoxidized Ac-L-Met-NHMe was achieved by reverse phase chromatography on a Delta-Pak C18 preparative column (19/300) (Waters) on a Waters HPLC system, equilibrated with H_2O and eluted with a linear gradient of acetonitrile from 0 to 55%. Ac-L-Met-*R,S*-SO-NHMe was eluted at 3% acetonitrile, whereas Ac-L-Met-NHMe was eluted at 30% acetonitrile. The fractions corresponding to Ac-L-Met-*R,S*-SO-NHMe were pooled and concentrated to eliminate acetonitrile. The proton NMR spectrum is in accord with the Ac-L-Met-*R,S*-SO-NHMe structure. Concentration of Ac-L-Met-*R,S*-SO-NHMe solution was determined on an analytic Atlantis C18 column (Waters) on an ÄKTA explorer system (Amersham Biosciences) by integrating the absorption peak at 215 nm (1 nmol of Ac-L-Met-*R,S*-SO-NHMe gives 1.62 area units).

Enzyme Kinetics. Kinetics studies were carried out with Ac-L-Met-*R,S*-SO-NHMe as a substrate and *E. coli* Trx1 as a reductant in the presence of a Trx-regenerating system (1.28 μM *E. coli* Trx reductase and 0.3 mM NADPH) as previously described by Olry et al. (*6*). The initial rate data were fit to the Michaelis−Menten relationship using least-squares analysis to determine k_{cat} and K_M with the program Sigmaplot (Jandel Scientific Software). All K_M values were determined at saturating concentrations of the other substrate.

Preparation of MsrB in the Disulfide State and Trx_{ox}. MsrB oxidation was achieved by mixing 100 μM MsrB with 300 mM MetSO in buffer A (50 mM Tris-HCl, 2 mM EDTA, pH 8). The MetSO used was D,L-Met-*R,S*-SO, of which only the R isomer is a substrate for MsrB (*6*). Trx oxidation was achieved by mixing 500 μM Trx with 1 mM DTNB in buffer A. After 10 min of incubation at room temperature, oxidized proteins were passed through an Econo-Pac 10 DG desalting column (Bio-Rad) equilibrated with buffer A. Oxidation of protein in the disulfide state was checked by titration with DTNB.

Fluorescence Properties of Wild-Type and Mutant MsrBs. The fluorescence characteristics of the wild-type MsrB in the reduced form ($MsrB_{red}$) and Cys-117/Cys-63 disulfide state, and the C63S MsrB in its reduced form and Cys-117 sulfenic acid state, were recorded on an spectrofluorometer (flx, SAFAS company) thermostated at 25 °C, in buffer A with 10 μM each protein.

Determination of the Rate of Ac-L-Met-NHMe Formation and of Thiol Loss by Single Turnover Quenched-Flow Experiments. Quenched-flow measurements were carried out at 25 °C on a SX18MV-R stopped-flow apparatus (Applied PhotoPhysics) fitted for the double-mixing mode and adapted to recover the quenched samples as previously described (*22*). Briefly, equal volumes (60 μL) of a solution containing 600 μM MsrB in 50 mM MES, pH 5.5, or in buffer A and a solution containing 700 mM Ac-L-Met-*R,S*-SO-NHMe in 50 mM MES, pH 5.5, or in buffer A were mixed in the aging loop. The mixture was then allowed to react for 30−800 ms before being mixed with an equal volume of a quenching aqueous solution containing 2% of trifluoroacetic acid. Quenched samples were then collected in a 200 μL loop. For each aging time, four shots were done, and the four corresponding quenched samples were pooled in a volume of 700 μL and then analyzed. Ac-L-Met-NHMe quantification in the quenched samples was carried out by reverse phase chromatography as described in the paragraph *Preparation of Ac-L-Met-R,S-SO-NHMe* by peak integration at 215 nm. The other part of the quenched samples was used to (1) determine the protein concentration from the absorbance at 280 nm and (2) quantify the free cysteine content, using 2,2′-dipyridyl disulfide as a thiol probe. Progress curves of pyridine-2-thione production were recorded at 343 nm in

buffer A. Enzyme concentration was 6.19 μM, and the 2,2′-dipyridyl disulfide concentration was 665 μM. The amount of pyridine-2-thione formed was calculated using an extinction coefficient at 343 nm of 8080 M^{-1} cm^{-1}. Data were plotted as mol of Ac-L-Met-NHMe formed per mol of MsrB and as free remaining thiols per mol of MsrB, both as a function of time. The rate of Ac-L-Met-NHMe formation was determined by fitting the curve to the monoexponential equation (eq 1), in which *a* represents the fraction of Ac-L-Met-NHMe formed per mol of MsrB and k_{obs} represents the rate constant.

$$y = a(1 - e^{-k_{obs}t}) \quad (1)$$

The rate of loss in free thiols was determined by fitting the curve to the monoexponential equation (eq 2) in which y_0 represents the number of free remaining thiols, *a* represents the number of oxidized thiols, and k_{obs} represents the rate constant.

$$y = y_0 + ae^{-k_{obs}t} \quad (2)$$

Kinetics of the Formation of the Cys-117 Sulfenic Acid Intermediate of C63S MsrB by Single Turnover Stopped-Flow Experiment. Kinetics of the C63S MsrB fluorescence decrease associated with the formation of the Cys-117 sulfenic acid intermediate were measured at 25 °C on a SX18MV-R stopped-flow apparatus (Applied PhotoPhysics) fitted for fluorescence measurements. The excitation wavelength was set at 291 nm, and the emitted light was collected using a 320 nm cutoff filter. One syringe contained MsrB in buffer A (10 μM, final concentration after mixing), and the other one contained Ac-L-Met-*R*,*S*-SO-NHMe at various concentrations in buffer A (5−550 mM, final concentration). An average of six runs was recorded for each Ac-L-Met-*R*,*S*-SO-NHMe concentration. Rate constants, k_{obs}, were obtained by fitting fluorescence traces with the monoexponential equation (eq 3) in which *c* represents the end point, *a* represents the amplitude of the fluorescence increase (<0), and k_{obs} represents the rate constant.

$$y = ae^{-k_{obs}t} + c \quad (3)$$

Data were fit to eq 4 using least-squares analysis to determine $k_{obs\ max}$ and *K* for Ac-L-Met-*R*,*S*-SO-NHMe. *S* represents the Ac-L-Met-*R*,*S*-SO-NHMe concentration, and *K* represents the K_s value for the substrate.

$$k_{obs} = k_{obs\ max}S/(K + S) \quad (4)$$

Kinetics of the Reduction of the Cys-117/Cys-63 MsrB Disulfide Bond by Trx by Single Turnover Stopped-Flow Experiments. Kinetic measurements of the Trx fluorescence quenching associated with the formation of the Cys-32/Cys-35 disulfide bond upon the reduction of the MsrB in the disulfide state ($MsrB_{ox}$) were carried out as previously described for MsrA (*22*). Briefly, the excitation wavelength was set at 310 nm, and the emitted light was collected above 320 nm using a cutoff filter. One syringe contained the $MsrB_{ox}$ in buffer A (from 10 to 25 μM, final concentration), and the other one contained the Trx in the reduced form (Trx_{red}) at various concentrations in buffer A (from 50 to 1250 μM, final concentration). An average of six runs was recorded for each concentration of Trx. Rate constants, k_{obs}, were obtained by fitting fluorescence traces with the monoexponential eq 2 with $a > 0$.

Data were fit to eq 5 using least-squares analysis to determine k_r, k_f, and *K* for Trx. *S* represents the Trx concentration, *K* represents the K_s value for Trx, and k_r and k_f represent the rate constants of the disulfide exchange in the reverse and forward directions, respectively.

$$MsrB_{ox} + Trx_{red} \overset{K}{\rightleftharpoons} [MsrB_{ox}\cdots Trx_{red}] \underset{k_r}{\overset{k_f}{\rightleftharpoons}} [MsrB_{red}\cdots Trx_{ox}]$$

$$k_{obs} = k_r + k_f\,S/(K + S) \quad (5)$$

Eq 5 was used, assuming that binding of Trx_{red} to $MsrB_{ox}$ is rapid equilibrium.

RESULTS AND DISCUSSION

Catalytic Constants with Ac-L-Met-R,S-SO-NHMe. The catalytic constants of *N. meningitidis* MsrB were determined with Ac-L-Met-*R*,*S*-SO-NHMe and Trx1 from *E. coli* as substrates and Trx reductase from *E. coli* and NADPH as the Trx-regenerating system. Ac-L-Met-*R*,*S*-SO-NHMe was used instead of MetSO because MsrB displays a better affinity for Ac-L-Met-*R*,*S*-SO-NHMe, and thereby, kinetic parameters of the reductase step could be determined at saturating concentration. K_M for Ac-L-Met-*R*,*S*-SO-NHMe and Trx and k_{cat} value at pH 8 and 5.5 were 2.2 ± 0.6 mM, 140 ± 22 μM, and 0.51 ± 0.06 s^{-1} and 7 ± 2 mM, 104 ± 26 μM, and 0.30 ± 0.04 s^{-1}, respectively. Doubling or halving the concentration of Trx reductase did not affect the k_{cat} value.

The fact that saturation kinetics were observed with a low K_M for Trx showed that Trx is a specific recycling reductant for MsrB similarly to that observed for *N. meningitidis* MsrA (*6*). Therefore, this suggests that specific interactions exist between Trx and Msrs. It is important to note that the affinity constant for Ac-L-Met-*R*,*S*-SO-NHMe has to be divided by 2, taking into account the fact that the isomer of MetSO is neither a substrate nor an inhibitor of MsrB (*6*).

Rate-Limiting Step Is Not Associated with the Concomitant Formation of the Sulfenic Acid Intermediate and of Ac-L-Met-NHMe. (A) Rate of Formation of Ac-L-Met-NHMe in the Wild-Type and C63S MsrBs. A means to determine the rate of formation of the sulfenic acid intermediate was to attain that of the Ac-L-Met-NHMe, which is formed concomitantly. To do so, the stopped-flow apparatus was adapted in a quenched-flow mode as previously described by Antoine et al. (*22*). At various times of incubation of MsrB with Ac-L-Met-*R*,*S*-SO-NHMe, in the absence of Trx, the reaction mixture was quenched by mixing it with trifluoroacetic acid. Ac-L-Met-NHMe was then quantified by reverse-phase chromatography analysis. The study was done at 350 mM Ac-L-Met-*R*,*S*-SO-NHMe, a concentration that can be considered to be saturating (see K_s value determined for C63S MsrB). At pH 8, a burst of Ac-L-Met-NHMe formation was observed with a stoichiometry of 0.9 and 0.8 mol of Ac-L-Met-NHMe/mol of wild-type and C63S MsrBs, respectively. However, the rate of the Ac-L-Met-NHMe formation was too fast, at least 50 s^{-1}, to be determined with the apparatus adapted for quenched-flow experiments, which gave a minimum aging time around 30 ms. In contrast, at pH 5.5, the rate was attainable, and the curve profile was fit to the

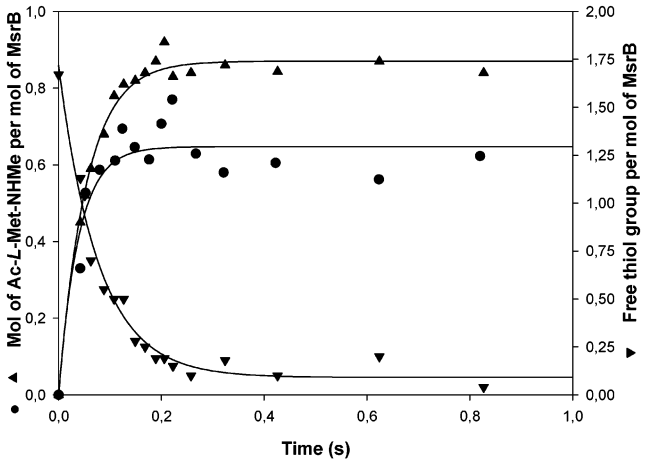

FIGURE 1: Time-resolved appearance of Ac-L-Met-NHMe for the wild type (▲) and C63S (●) MsrBs from *N. meningitidis* and disappearance of free thiols for the wild type (▼) under single turnover kinetics. The quenched-flow experiment was carried out at 25 °C in 50 mM MES, pH 5.5 as described in the Experimental Procedures. Symbols represent experimental data points (▲ for Ac-L-Met-NHMe quantification, ▼ for free thiol titration for the wild type, and ● for Ac-L-Met-NHMe for the C63S MsrB). Data of Ac-L-Met-NHMe quantification were fit to eq 1 and gave rate constants of 18 ± 1 and 23 ± 3 s^{-1} with amplitudes of 0.87 ± 0.01 mol of Ac-L-Met-NHMe per mol of enzyme and 0.65 ± 0.02 mol of Ac-L-Met-NHMe per mol of enzyme for the wild type and C63S MsrBs, respectively. Data of free thiol titration were fit to eq 2 and gave a rate constant of 13 ± 1 s^{-1} with amplitude of 1.82 ± 0.07 free thiol groups per mol of enzyme for the wild type.

monoexponential eq 1 with k_{obs} values of 18 and 23 s^{-1} and a stoichiometry of 0.87 and 0.65 mol of Ac-L-Met-NHMe/mol of wild-type and C63S MsrBs, respectively (Figure 1). The fact that a stoichiometry of only 0.8 and 0.65 mol of Ac-L-Met-NHMe/mol of C63S MsrB was found at pH 8 and pH 5.5, respectively, remains to be explained. A possibility was that MsrB in the sulfenic acid state and reduced MsrB ($MsrB_{red}$) reacted together to form a dimer and thus decreased the concentration of C63S MsrB. In fact, it is not the case because on nonreducing gels, no significant amount of dimer was observed (gels not shown).

As expected, substituting Ser for Cys-63 has no significant effect on the rate of formation of Ac-L-Met-NHMe. More importantly is the fact that the rates of the reductase step for the wild-type and C63S MsrBs are at least 60-fold higher than the k_{cat} value determined for the wild type under steady-state conditions and at the same pH of 5.5.

(B) Rate of Formation of the Sulfenic Acid Intermediate in the C63S MsrB. Another approach to determine the rate of formation of the sulfenic acid intermediate was to follow a specific message associated with the oxidation of the catalytic cysteine. As shown next, the probe used was Trp-65 whose fluorescence emission intensity at 343 nm decreases upon going from the reduced to the sulfenic acid forms. The study was done with the C63S MsrB, which accumulates the sulfenic acid intermediate but not with the wild type, which accumulates the disulfide intermediate in the absence of Trx (see next paragraph).

As shown in Figure 2A, wild-type $MsrB_{red}$ presented a maximum excitation wavelength at 291 nm and a fluorescence emission maximum at <320 nm with a shoulder at 343 nm. This suggested a contribution of tyrosine and of tryptophan residues to the fluorescence signal at <320 and

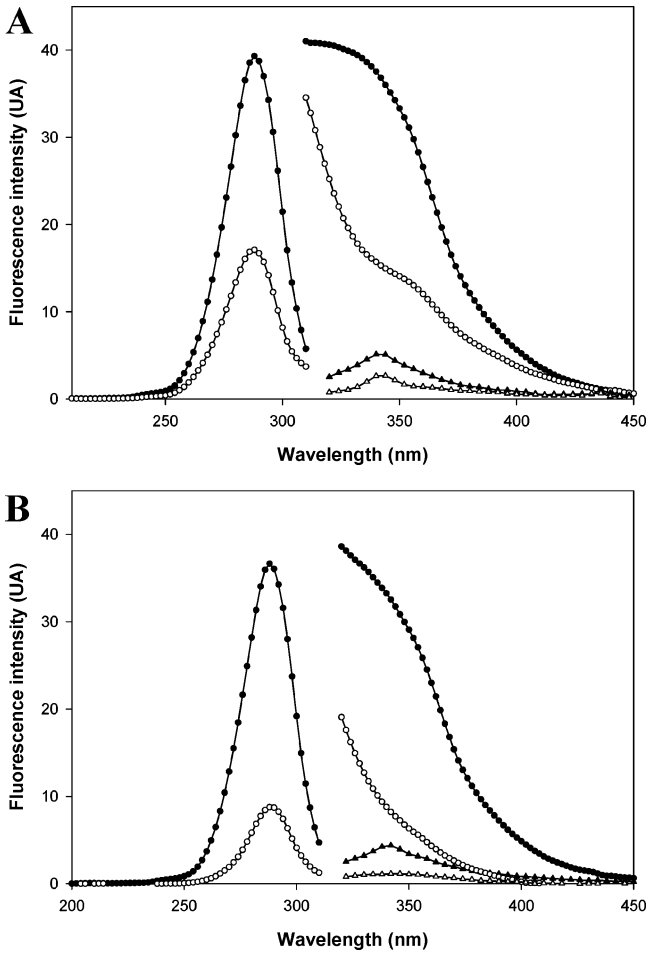

FIGURE 2: Fluorescence spectra of *N. meningitidis* wild-type $MsrB_{red}$ and $MsrB_{ox}$ and of *N. meningitidis* C63S MsrB in reduced and sulfenic acid states. All the spectra were recorded with 10 μM protein at 25 °C in buffer A, pH 8. In panel A, the wild type: excitation spectra of $MsrB_{red}$ (●) and $MsrB_{ox}$ (○) (emission followed at 340 nm), emission spectra of $MsrB_{red}$ (●) and $MsrB_{ox}$ (○) (excitation at 291 nm) and $MsrB_{red}$ (▲) and $MsrB_{ox}$ (△) (excitation at 310 nm). In panel B, the C63S MsrB: excitation spectra of $MsrB_{red}$ (●) and MsrB sulfenic acid form (○) (emission followed at 340 nm), emission spectra of $MsrB_{red}$ (●) and MsrB sulfenic acid form (○) (excitation at 291 nm), and emission spectra of $MsrB_{red}$ (▲) and MsrB sulfenic acid form (△) (excitation at 310 nm).

343 nm, respectively. In MsrB from *N. meningitidis*, there are nine tyrosines and one tryptophan at position 65. The fact that in W65F MsrB, the fluorescence emission strongly decreased at >320 nm with a disappearance of the shoulder at 343 nm when the excitation was done at 291 nm confirmed the contribution of only Trp-65 in the fluorescence emission at 343 nm (spectrum not shown). Inspection of the X-ray structure shows that Trp-65 is situated in a loop near the catalytic Cys-117 and has recently been shown to be implicated in the binding of the methyl group of the substrate (data not shown). Thus, Trp-65 could be a good candidate to probe a change of the active site environment along the reductase process.

This was shown on the C63S MsrB, which accumulates the sulfenic acid intermediate. When excited at 291 nm, C63S MsrB in a sulfenic acid state showed a fluorescence emission at 343 nm that decreased by a factor of 50% (integrated from 320 to 450 nm) when compared with that of the $MsrB_{red}$ (Figure 2B). Therefore, the presence of a sulfenic acid on

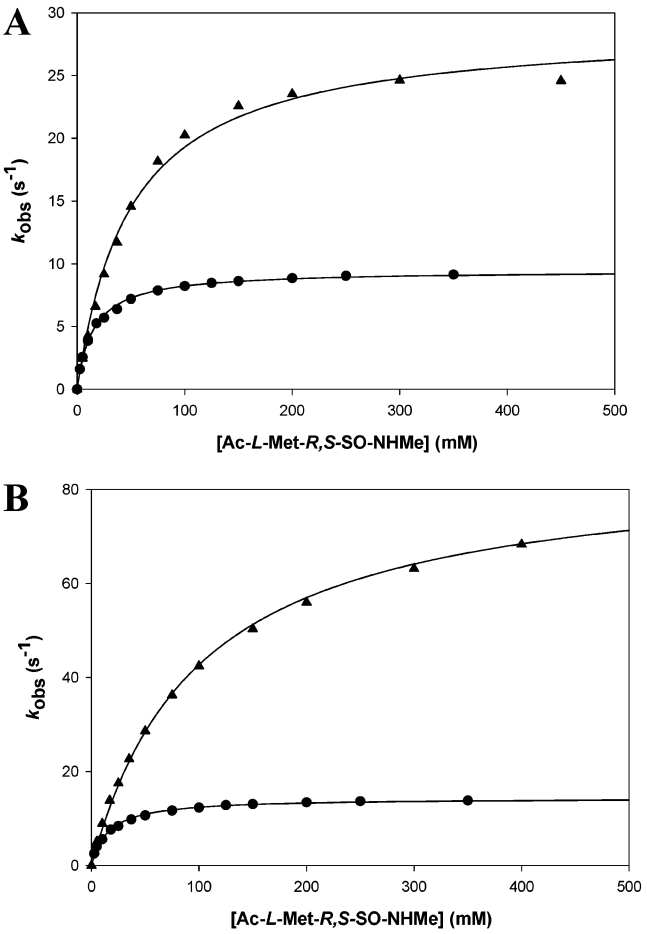

FIGURE 3: Determination of the catalytic parameters of the reductase step of wild type (A) and C63S MsrB (B) from *N. meningitidis* in buffer A pH 8 (▲) and in MES buffer pH 5.5 (●) measured by fluorescence stopped-flow under single turn-over kinetics. The MsrB fluorescence decrease was recorded on a stopped-flow apparatus at 25 °C. Final concentration of wild-type and C63S MsrBs was 10 μM. Excitation wavelength was set at 291 nm, and emitted light was collected above 320 nm using a cutoff filter. Data were fit to eq 4, which gave $k_{obs\ max}$ and K_s values of 28.9 ± 0.7 s^{-1} and 49 ± 4 mM and 9.5 ± 0.1 s^{-1} and 15 ± 1 mM for the wild type in buffer A and in 50 mM MES buffer pH 5.5, respectively, and 85 ± 1 s^{-1} and 101 ± 4 mM and 14.3 ± 0.3 s^{-1} and 15 ± 1 mM for the C63S MsrB in buffer A, pH 8, and in 50 mM MES buffer pH 5.5, respectively.

the catalytic Cys-117 likely modifies locally the Trp-65 environment, leading to a quenching of its fluorescence emission message. At pH 8 and 5.5, a fast decrease of the fluorescence signal of the C63S MsrB was observed with the Ac-L-Met-*R,S*-SO-NHMe concentrations used. All the curves fitted to the monoexponential eq 2 with k_{obs} values ranging from 1 to 70 s^{-1}. From the curve of k_{obs} versus substrate concentration, K_s values of 101 and 15 mM for Ac-L-Met-*R,S*-SO-NHMe and $k_{obs\ max}$ values of 85 and 14.3 s^{-1} were determined at pH 8 and 5.5, respectively (Figure 3B). The k_{obs} values determined at pH 8 and 5.5 are 163- and 48-fold higher than those determined under steady-state conditions for the wild type, respectively.

Therefore, it can be concluded that the rate of the reductase process determined by the two approaches (i.e., by following the rate of formation of either Ac-L-Met-NHMe or the sulfenic acid intermediate) is largely higher than the k_{cat}. This demonstrates that the rate-limiting step in MsrB takes place after the formation of the sulfenic acid intermediate and is associated with either the Cys-117/Cys-63 disulfide bond formation or the Trx reduction process.

Rate of Formation of the Cys-117/Cys-63 MsrB Disulfide Bond Is Not Rate-Limiting and Is as Fast as That of Sulfenic Acid Intermediate and Met Formations. One approach is to determine the rate of the intradisulfide bond formation in the wild type by following a specific message associated with its formation, such as a modification of the Trp-65 fluorescence emission intensity, provided that the message can be differentiated from that observed upon formation of the sulfenic acid intermediate. In fact, a quenching of the Trp-65 emission fluorescence intensity due to formation of the Cys-117/Cys-63 disulfide bond is also observed and is moreover similar to that observed upon formation of the sulfenic acid intermediate in the C63S MsrB (Figure 2B). Moreover, K_s for Ac-L-Met-*R,S*-SO-NHMe and the $k_{obs\ max}$ values of the wild-type MsrB at pH 8 and 5.5 determined by following the quenching of the Trp-65 fluorescence are in the same range as those determined for the C63S MsrB (Figure 3A and data in legend of Figure 3A). Consequently, it was not possible to attain the rate of the disulfide bond formation using Trp-65 as a fluorescent probe.

Therefore, there remained only one method to determine the rate of formation of the Cys-117/Cys-63 MsrB disulfide bond. It was to follow the loss of the two free thiol groups by quenched-flow experiments. Indeed, the Cys-117 free thiol group is lost first in the reductase step, whereas the Cys-63 free thiol group is lost only in the second step, which leads to formation of the Cys-117/Cys-63 MsrB disulfide bond. This analysis was done with the samples obtained from the quenched-flow experiments described previously. At pH 5.5 and with 350 mM Ac-L-Met-*R,S*-SO-NHMe, the curve profile was fit to the monoexponential eq 2, with a concomitant loss of two cysteines and a k_{obs} value of 13 s^{-1} (Figure 1). The fact that the k_{obs} value was in the range of that determined by following Ac-L-Met-NHMe formation with the wild type and the C63S MsrBs as well suggested that as soon as Cys-117 is oxidized in the sulfenic acid form in the wild-type, Cys-63 attacks it and forms a disulfide bond. In other words, the rate of the nucleophilic attack of Cys-63 on the Cys-117 sulfenic intermediate is limited by that determining the formation of the sulfenic acid intermediate, which as a consequence cannot accumulate. Therefore, the rate-limiting step in MsrB takes place after the Cys-117/Cys-63 disulfide bond formation, and the rate-determining step in the formation of the disulfide bond is governed by that leading to formation of the sulfenic acid intermediate.

Rate-Limiting Step Probably Takes Place within the Trx-Recycling Process After the Two-Electron Chemical Exchange. The rate of formation of the Trx_{ox} was determined by following the decrease of the Trx fluorescence intensity upon going from Trx_{red} to Trx_{ox} during the reduction of the Cys-117/Cys-63 disulfide bond of the MsrB. To interpret the data, we should first verify that the change in the fluorescence signal of the MsrB upon going from the oxidized disulfide to the reduced forms did not interfere with the Trx message. As shown in Figure 4, when the excitation wavelength was set at 310 nm, the fluorescence message of MsrB increases upon going from $MsrB_{ox}$ to $MsrB_{red}$. Therefore, the decrease in fluorescence intensity corresponded to a change in the fluorescence message of the Trx. Under the experimental conditions used, at pH 8, the

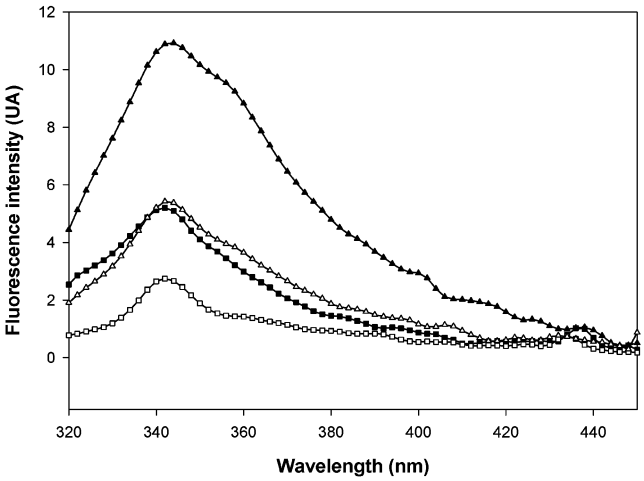

FIGURE 4: Fluorescence emission spectra of the *E. coli* Trx_{red} and Trx_{ox} and of the *N. meningitidis* $MsrB_{red}$ and $MsrB_{ox}$. Fluorescence spectra of 10 μM $MsrB_{red}$ (■) and $MsrB_{ox}$ (□) and 10 μM Trx_{red} (▲) and Trx_{ox} (△) were recorded at 25 °C on excitation at 310 nm.

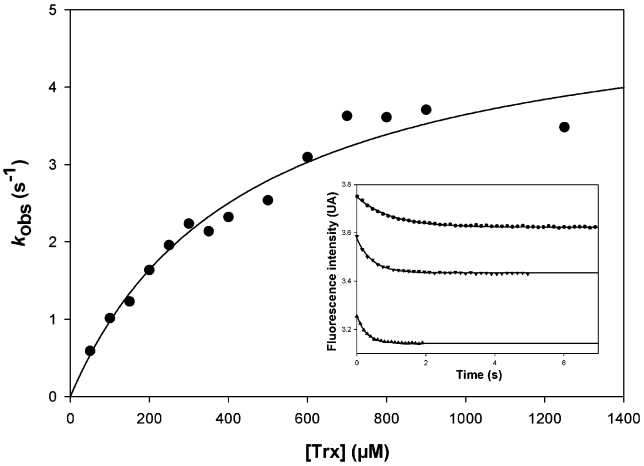

FIGURE 5: Rate of reduction of the Cys-117/Cys-63 disulfide bond of the *N. meningitidis* MsrB by *E. coli* Trx measured by fluorescence stopped-flow experiments. The Trx fluorescence quenching associated with Trx disulfide bond formation was recorded on a stopped-flow apparatus at 25 °C in buffer A pH 8 by mixing Trx_{red} and $MsrB_{ox}$. MsrB final concentration varied from 10 to 25 μM. Excitation wavelength was set at 310 nm, and emitted light was collected above 320 nm using a cutoff filter. Data were fit to eq 5, which gave k_f, k_r, and K_s values of 5.2 ± 0.4 s^{-1}, $1 \times 10^{-3} \pm 3 \times 10^{-1}$ s^{-1}, and 440 ± 75 μM, respectively. Symbols (●) represent experimental data points. Inset: representative sampling of primary data: 10 μM $MsrB_{ox}$ and 100 μM Trx_{red} (●), 15 μM $MsrB_{ox}$ and 300 μM Trx_{red} (▼), and 25 μM $MsrB_{ox}$ and 800 μM Trx_{red} (▲). Data were fit to eq 2 with $a > 0$, which gave k_{obs} of 1.01 ± 0.01, 2.23 ± 0.02, and 3.64 ± 0.01 s^{-1} at 100, 300, and 800 μM Trx, respectively.

concentration of the Cys-117/Cys-63 disulfide MsrB varied from 10 to 25 μM, and the concentration of the Trx_{red} varied from 50 to 1250 μM. For each concentration of Trx, a k_{obs} value was determined. Assuming binding of Trx_{red} to $MsrB_{ox}$ is rapid equilibrium and using eq 5, a K_s value of 440 μM for Trx and k_f and k_r values of 5.2 and $\sim$0 s^{-1} can be determined from the curve k_{obs} versus Trx concentration, respectively (Figure 5). The fact that the curve passes through the origin indicates that, in first approximation, the recycling process going up to disulfide exchange can be considered as irreversible; therefore, the k_{obs} value is presumably measuring the rate of the chemical reaction. The values of K_s and k_f are 3.2- and 10-fold higher than the K_M and k_{cat} values determined under steady-state conditions in which the Trx-reductase recycling system was assumed to not be rate-limiting. To confirm that the k_{cat} value obtained with the Trx-reductase recycling system was indeed measured under steady-state conditions, the k_{cat} value was also determined by following the rate of Ac-L-Met-NHMe formation in the absence of Trx reductase, at saturating concentration of Ac-L-Met-*R*,*S*-SO-NHMe and Trx. The rate was 1.3 s^{-1}. A rate constant of 1 s^{-1} was obtained when reduction of $MsrB_{ox}$ by Trx_{red} was carried out in the presence of Trx reductase by following NADPH disappearance (experiments not shown). In both cases, the rate constants are in the range of that determined under steady-state conditions in the presence of Trx reductase. Therefore, the fact that the k_{cat} value is significantly lower than the k_f value strongly supports a rate-limiting step within the Trx-recycling process that takes place after the two-electron chemical exchange and thus is associated with release of Trx_{ox}. In this context, release of Trx_{ox} could be rate limited by a conformational change of the $MsrB_{red}/Trx_{ox}$ complex. If so, it is probable that a similar conformational change of the $MsrB_{ox}/Trx_{red}$ complex also takes place after formation of the Michaelis complex. This latter conformational change could be rate-determining in the formation of the $MsrB_{red}/Trx_{ox}$ complex. Further studies including methods to directly investigate MsrB/Trx binding kinetics should be done to settle such hypotheses.

CONCLUSION

We have shown that (1) the rate-limiting step in MsrB is within the Trx-recycling process and probably takes place after the two-electron chemical exchange and (2) the formation of the sulfenic acid intermediate is rate determining within the two-step process leading to formation of the intradisulfide Cys-117/Cys-63 intermediate. As already mentioned, the active sites of MsrA and MsrB are structurally different. In particular, the amino acids involved in the activation of the reductase step are different. This includes the amino acids implicated in (1) the decrease of the pK_a of the catalytic cysteine, (2) the increase of the electrophilic character of the sulfoxide, and (3) the 1,3-sigmatropic rearrangement that leads to formation of the sulfenic acid intermediate. Compared to that of the *N. meningitidis* MsrA, the rate of the reductase step that leads to the sulfenic acid intermediate at pH 8 is 20-fold slower in MsrB (*22*). This remains to be explained but likely reflects differences in the nature of the amino acids of the two active sites involved either in the catalysis or in the substrate recognition.

The fact that the rate-limiting step within the Trx-recycling process probably takes place after the two-electron chemical process in MsrB raises the question as to whether the structurally unrelated MsrA behaves similarly. The data recently published by our group on the MsrA from *N. meningitidis* have clearly shown that the Trx-recycling process is rate limiting. But no definitive conclusion was given on which step was rate limiting within the Trx process (*22*). Interpreting now the experimental data published and by comparison with those from MsrB, it can be concluded that MsrA likely behaves similarly to MsrB. Indeed, under single turnover conditions, at pH 8, using eq 5, the K_s constant of MsrA for Trx and the k_f and k_r values determined

from the curve k_{obs} versus Trx concentration were 930 μM, 50 s^{-1}, and $\sim$0 s^{-1}, respectively, whereas under steady-state conditions the K_M for Trx and the k_{cat} constant were 75 μM and 7 s^{-1}, respectively (*22*). Therefore, the rate limiting step for MsrA probably also takes place after the two-electron chemical exchange. Consequently, release of Trx_{ox} is likely rate limiting for both MsrA and MsrB from *N. meningitidis*.

Msrs represent an interesting example of convergent evolution in which two structurally unrelated proteins have evolved to catalyze the same reaction with the same chemical and kinetic mechanisms but with an opposite MetSO stereoselectivity. Studies are presently underway to characterize all the amino acids of the MsrA and MsrB from *N. meningitidis*, which are involved not only in the chemical activation of the three steps but also in the substrate specificities.

ACKNOWLEDGMENT

We are very grateful to Dr. F. Barras for the gift of the BE002 strain, to A. Kriznik for Ac-L-Met-*R*,*S*-SO-NHMe synthesis and purification, to Dr. A. Van Dorsselaer for mass determination, to Dr. E. McRae for careful reading of the manuscript, and to Dr. W. Wallace Cleland, University of Wisconsin, Madison, for critically reading the manuscript.

REFERENCES

1. Brot, N., Weissbach, L., Werth, J., and Weissbach, H. (1981) Enzymatic reduction of protein-bound methionine sulfoxide, *Proc. Natl. Acad. Sci. U.S.A. 78*, 2155−2158.
2. Moskovitz, J., Poston, J. M., Berlett, B. S., Nosworthy, N. J., Szczepanowski, R., and Stadtman, E. R. (2000) Overexpression of peptide−methionine sulfoxide reductase in *Saccharomyces cerevisiae* and human T cells provides them with high resistance to oxidative stress, *J. Biol. Chem. 275*, 14167−14172.
3. Sharov, V. S., Ferrington, D. A., Squier, T. C., and Schoneich, C. (1999) Diastereoselective reduction of protein-bound methionine sulfoxide by methionine sulfoxide reductase, *FEBS Lett. 455*, 247−250.
4. Moskovitz, J., Singh, V. K., Requena, J., Wilkinson, B. J., Jayaswal, R. K., and Stadtman, E. R. (2002) Purification and characterization of methionine sulfoxide reductases from mouse and *Staphylococcus aureus* and their substrate stereospecificity, *Biochem. Biophys. Res. Commun. 290*, 62−65.
5. Grimaud, R., Ezraty, B., Mitchell, J. K., Lafitte, D., Briand, C., Derrick, P. J., and Barras, F. (2001) Repair of oxidized proteins. Identification of a new methionine sulfoxide reductase, *J. Biol. Chem. 276*, 48915−48920.
6. Olry, A., Boschi-Muller, S., Marraud, M., Sanglier-Cianferani, S., Van Dorsselear, A., and Branlant, G. (2002) Characterization of the methionine sulfoxide reductase activities of PILB, a probable virulence factor from *Neisseria meningitidis*, *J. Biol. Chem. 277*, 12016−12022.
7. Levine, R. L., Moskovitz, J., and Stadtman, E. R. (2000) Oxidation of methionine in proteins: roles in antioxidant defense and cellular regulation, *IUBMB Life 50*, 301−307.
8. Levine, R. L., Berlett, B. S., Moskovitz, J., Mosoni, L., and Stadtman, E. R. (1999) Methionine residues may protect proteins from critical oxidative damage, *Mech. Ageing Dev. 107*, 323−332.
9. Brot, N., and Weissbach, H. (2000) Peptide methionine sulfoxide reductase: biochemistry and physiological role, *Biopolymers 55*, 288−296.
10. Stadtman, E. R., Moskovitz, J., and Levine, R. L. (2003) Oxidation of methionine residues of proteins: biological consequences, *Antioxid. Redox. Signal 5*, 577−582.
11. Moskovitz, J., Flescher, E., Berlett, B. S., Azare, J., Poston, J. M., and Stadtman, E. R. (1998) Overexpression of peptide−methionine sulfoxide reductase in *Saccharomyces cerevisiae* and human T cells provides them with high resistance to oxidative stress, *Proc. Natl. Acad. Sci. U.S.A. 95*, 14071−14075.
12. Wizemann, T. M., Moskovitz, J., Pearce, B. J., Cundell, D., Arvidson, C. G., So, M., Weissbach, H., Brot, N., and Masure, H. R. (1996) Peptide methionine sulfoxide reductase contributes to the maintenance of adhesins in three major pathogens, *Proc. Natl. Acad. Sci. U.S.A. 93*, 7985−7990.
13. Hassouni, M. E., Chambost, J. P., Expert, D., Van Gijsegem, F., and Barras, F. (1999) The minimal gene set member *msrA*, encoding peptide methionine sulfoxide reductase, is a virulence determinant of the plant pathogen *Erwinia chrysanthemi*, *Proc. Natl. Acad. Sci. U.S.A. 96*, 887−892.
14. Dhandayuthapani, S., Blaylock, M. W., Bebear, C. M., Rasmussen, W. G., and Baseman, J. B. (2001) Peptide methionine sulfoxide reductase (MsrA) is a virulence determinant in *Mycoplasma genitalium*, *J. Bacteriol. 183*, 5645−5650.
15. Tete-Favier, F., Cobessi, D., Boschi-Muller, S., Azza, S., Branlant, G., and Aubry, A. (2000) Crystal structure of the *Escherichia coli* peptide methionine−sulphoxide reductase at 1.9 Å resolution, *Structure Fold. Des. 8*, 1167−1178.
16. Lowther, W. T., Brot, N., Weissbach, H., and Matthews, B. W. (2000) Structure and mechanism of peptide methionine sulfoxide reductase, an antioxidation enzyme, *Biochemistry 39*, 13307−13312.
17. Lowther, W. T., Weissbach, H., Etienne, F., Brot, N., and Matthews, B. W. (2002) The mirrored methionine sulfoxide reductases of *Neisseria gonorrhoeae* pilB, *Nat. Struct. Biol. 9*, 348−352.
18. Kauffmann, B., Favier, F., Olry, A., Boschi-Muller, S., Carpentier, P., Branlant, G., and Aubry, A. (2002) Crystallization and preliminary X-ray diffraction studies of the peptide methionine sulfoxide reductase B domain of *Neisseria meningitidis* PILB, *Acta Crystallogr., Sect. D 58*, 1467−1469.
19. Taylor, A. B., Benglis, D. M., Jr., Dhandayuthapani, S., and Hart, P. J. (2003) Structure of *Mycobacterium tuberculosi*s methionine sulfoxide reductase A in complex with protein-bound methionine, *J. Bacteriol. 185*, 4119−4126.
20. Boschi-Muller, S., Azza, S., Sanglier-Cianferani, S., Talfournier, F., Van Dorsselear, A., and Branlant, G. (2000) A sulfenic acid enzyme intermediate is involved in the catalytic mechanism of peptide methionine sulfoxide reductase from *Escherichia coli*, *J. Biol. Chem. 275*, 35908−35913.
21. Boschi-Muller, S., Azza, S., and Branlant, G. (2001) *Escherichia coli* methionine sulfoxide reductase with a truncated N terminus or C terminus, or both, retains the ability to reduce methionine sulfoxide, *Protein Sci. 10*, 2272−2279.
22. Antoine, M., Boschi-Muller, S., and Branlant, G. (2003) Kinetic characterization of the chemical steps involved in the catalytic mechanism of methionine sulfoxide reductase A from *Neisseria meningitidis*, *J. Biol. Chem. 278*, 45352−45357.
23. Mossner, E., Huber-Wunderlich, M., and Glockshuber, R. (1998) Characterization of *Escherichia coli* thioredoxin variants mimicking the active sites of other thiol/disulfide oxidoreductases, *Protein Sci. 7*, 1233−1244.
24. Mulrooney, S. B. (1997) Application of a single-plasmid vector for mutagenesis and high-level expression of thioredoxin reductase and its use to examine flavin cofactor incorporation, *Protein Expr. Purif. 9*, 372−378.

BI049306Z